

Electric-field-induced second-harmonic generation in GaN devices

Kristen A. Peterson and Daniel J. Kane

Southwest Sciences, Inc., Suite E-11, 1570 Pacheco Street, Santa Fe, New Mexico 87505

Received October 4, 2000

Electric-field-induced second-harmonic generation is used to detect electric fields in a GaN UV Schottky photodiode and in a GaN light-emitting diode. The second-harmonic signal is measured as a function of bias voltage and incident laser power. This technique is sensitive to small applied voltages and can be used to track electronic waveforms. The photocurrent generated by this technique is found to be less than 100 pA when the fundamental and second-harmonic frequencies are both below the device bandgap. © 2001 Optical Society of America

OCIS codes: 190.1900, 190.5970, 300.6420.

Second-harmonic (SH) generation through a second-order optical effect requires a material that lacks inversion symmetry or a symmetry-breaking interface. However, the presence of an electric field can permit SH generation through a third-order process called electric-field-induced second-harmonic (EFISH) generation. Because third-order susceptibilities $\chi^{(3)}$ are typically small, large voltages and peak laser powers are needed to make EFISH observable. Whereas voltages in semiconductors comprise only a few volts, the voltage drop occurs over a narrow depletion region where electric fields can be as high as 10^6 V/cm in some devices. As a result, the large electric fields that are present in semiconductors, together with the comparatively large values of $\chi^{(3)}$ of semiconductors, make this otherwise weak effect observable.

Indeed, EFISH generation has been observed at metal–semiconductor (silicon) junctions,¹ at silicon–silicon oxide interfaces,^{2–5} and in GaAs–AlGaAs quantum wells.⁶ It has also been used to measure wave propagation in silicon waveguides.⁷ However, in all those studies the probe laser was above the bandgap of the material (800 nm–1 μ m), producing large carrier concentrations and limiting probe beam penetration.

In this study we use fundamental and SH frequencies below the device bandgap. This approach is less disruptive because fewer carriers are created by photon absorption. Greater penetration of the probe beam opens the possibility of probing points hundreds of micrometers deep in an integrated circuit. We observe EFISH generation from the active region of a GaN UV Schottky diode photodetector (APA Optics) and a GaN light-emitting diode (LED; Nichia Corporation) with bandgaps greater than 400 nm. We take advantage of near-resonance enhancement at the SH while reducing absorption by probing with a Ti:sapphire laser tuned below one half of the bandgap. Ultimately, we hope to use this technique to probe silicon-based integrated circuits by using infrared laser light near 2 μ m.

Figure 1 is a schematic of the EFISH apparatus. The probe laser beam is focused onto a semiconductor sample to a spot size of ~ 50 - μ m. (Much higher spatial resolution can be achieved by tighter focusing and by use of confocal optics.) A half-wave plate and a polar-

izer are used for variable attenuation and polarization control of the probe beam. The probe beam is incident at 45° to the sample surface. The SH signal, copropagating with the specular probe beam, is directed through a 0.25-m spectrometer. UV pass-visible-blocking filters in front of the spectrometer block any residual fundamental. The signal can be directed to either of two spectrometer exit ports: a monochromator port with a slit and phototube for intensity measurements at specific wavelengths and an imaging port with a cooled CCD camera to obtain spectra of the SH signal. The polarization of the reflected beam is rotated by mirror to 45° relative to the grating axis, so grating efficiencies can be ignored. A dual-modulation technique is used to remove any non-electric-field-dependent signal. The applied voltage waveform and the chopped laser beam are at different, locked frequencies, and the EFISH signal is detected at the sum frequency. A microscope objective and a CCD camera above the sample are used to view the probe beam alignment. A picoameter (not shown), connected directly to the otherwise isolated device, monitors photoinduced current.

Figure 2 illustrates the semiconductor devices. An image of a GaN LED similar to the one used here is shown in Fig. 2a, and a drawing of the photodiode is shown in Fig. 2b. The UV LED has an emission

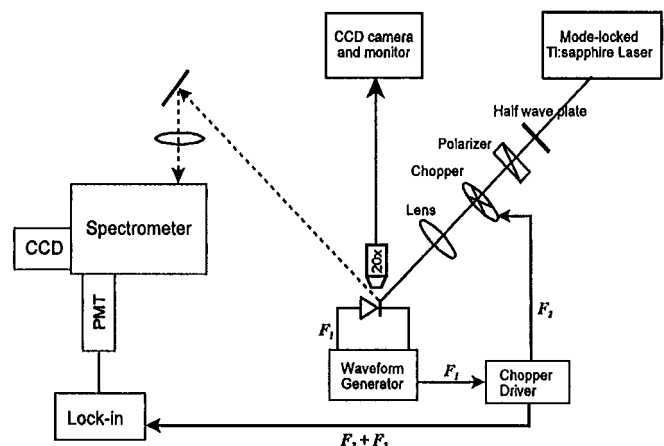


Fig. 1. Schematic of apparatus for EFISH generation and detection. PMT, photomultiplier tube.

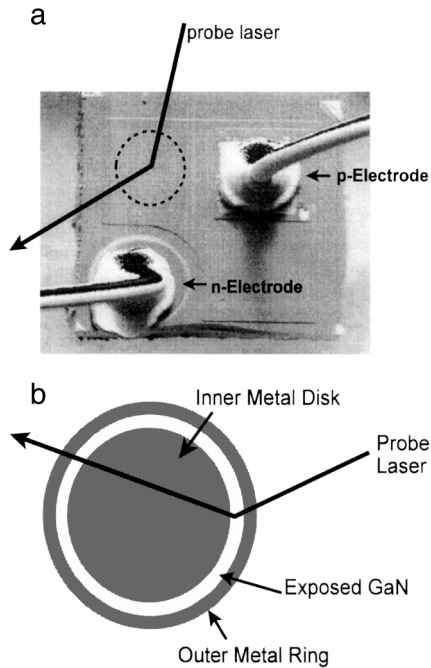


Fig. 2. GaN devices used in this study. a, Image of a GaN blue LED from Ref. 9, p. 302. Used by permission. b, Drawing of the GaN Schottky photodiode as observed through a $10\times$ objective.

wavelength of 370 nm. We believe that this is a single-quantum-well device, although the exact structure is proprietary. Published structures of similar LED's show the quantum-well layers parallel to the top surface under a p -GaN layer approximately $0.1\text{--}0.2\ \mu\text{m}$ thick.^{8,9} The Schottky photodiode is sensitive from 200 to 365 nm, with a sharp cutoff at 365 nm. Its active surface consists of a central metal disk, an exposed ring consisting of a thin layer of GaN grown upon sapphire, and an outer metal ring. A SH signal is observed only when the laser is focused onto the exposed GaN. Moving the sample so the beam focuses on the metallized surface on either side results in no SH generation.

Figures 3(a) and 3(b) show the dependence of the magnitude of the EFISH signal on the magnitude of the bias voltage for the two devices. The center frequency of the laser is 797 nm; thus the doubled frequency is below the bandgap of each device. The average power, chopped at 1 kHz, is 100 mW at the sample. A signal at zero bias [see Figs. 3(c) and 3(d)] is removed by the dual-modulation technique. Spectrally resolved signals (data not shown) peak at twice the probe laser frequency, confirming that they are due to the SH and not to luminescence. Figures 3(a) and 3(b) show an increasing EFISH signal with increasing reverse bias voltage. The magnitude of the EFISH signal increases with applied voltage but is out of phase with the signal observed at zero bias (see Fig. 4). At zero applied voltage, a significant SH signal is observed at the laser chopping frequency. Figures 3(c) and 3(d) show the dependence of the signal on fundamental laser power at zero bias. Data were taken for two polarization conditions, S_{in} and P_{in} , with no polar-

ization selection on the SH signal. The dependence on laser power is parabolic (solid lines), as expected for a second-order process. We did not attempt to determine experimentally the cause of the SH at zero applied bias, but there are three possible sources: (1) GaN is noncentrosymmetric, and the SH can be generated in the bulk without the presence of an electric field. (2) The SH can be generated from the

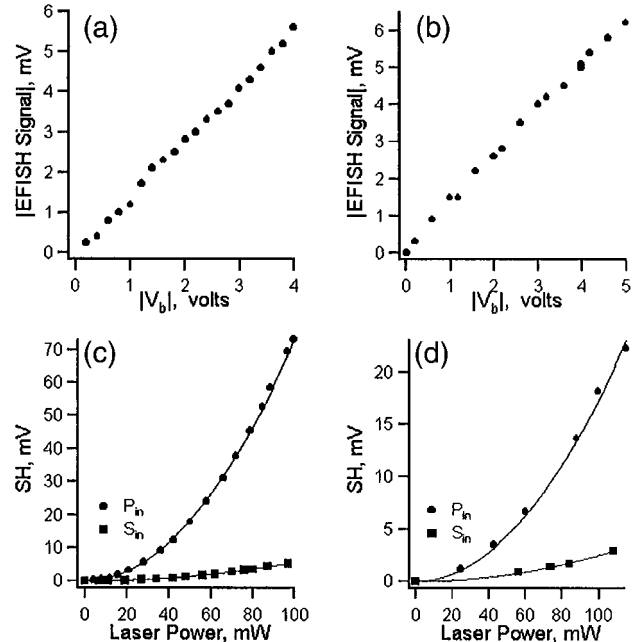


Fig. 3. Magnitude of the EFISH signal with change in the magnitude of the reverse bias voltage, $|V_b|$, at constant probe laser power for (a) the LED and (b) the photodiode. Probe laser power dependence of the SH background signal at $V_b = 0$ for (c) the LED and (d) the photodiode.

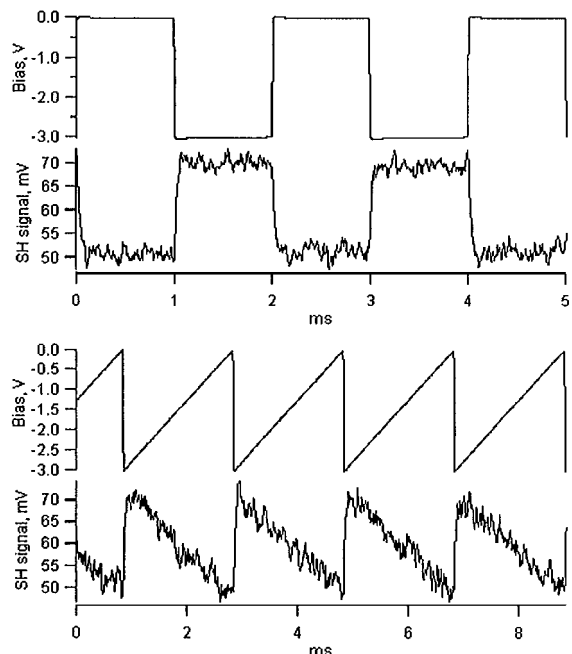


Fig. 4. Tracking of reverse-bias waveforms across the GaN LED. The 70-mV background SH is not removed from the signal, and the phase difference between the EFISH and the background SH is apparent.

surface. Surface SH signals are typically much weaker than bulk SH signals. (3) GaN-based semiconductors are piezoelectric. Lattice mismatch produces strain that causes an electric field to be generated. These devices are based on GaN grown upon sapphire where the lattice mismatch, 14.8%, can produce piezoelectric fields of the order of 500 kV/cm (see Ref. 9, Chap. 4). These piezoelectric field magnitudes are of the order of the waveform-induced fields at the p-n junction. We believe that much of the signal present at zero bias is due to EFISH from a strain-induced piezoelectric field.

For both the Schottky photodiode and the LED, the voltage dependence of the EFISH is linear with applied voltage [Figs. 3(a) and 3(b)]. In general, we expect EFISH intensity to be quadratic in applied bias voltage according to

$$I_{2\omega} \propto P_{2\omega}^2 \propto |\chi^{(3)} E_{\omega}^2 E_v|^2, \quad (1)$$

where $I_{2\omega}$ is the SH intensity and $P_{2\omega}$ is the polarization at the SH. $\chi^{(3)}$ is the third-order nonlinear susceptibility, E_{ω} is the electric field of the probe laser beam, and E_v is the applied electric field across the junction. With background SH present, the total SH intensity becomes

$$I_{2\omega} \propto |P_v + P_b|^2 = P_v^2 + 2P_v P_b + P_b^2, \quad (2)$$

where P_v is the EFISH polarization given by relation (1) and P_b is the background SH polarization. P_b could be a piezoelectric term when $P_b \propto \chi^{(3)} E_{\omega}^2 E_{\text{piezo}}$ or a second-order term for $P_b \propto \chi^{(2)} E_{\omega}^2$. Regardless of the source of the background term, if $P_b \gg P_v$, homodyne detection of P_v becomes possible through the $2P_v P_b$ term. This homodyne interaction produces the linear dependence of the EFISH intensity on applied voltage. The advantage of homodyne detection when an ac measurement is being made (as was done here because the bias voltage is modulated) is that a large coherent background can effectively amplify small signals. Normally P_v is small, but, with the addition of the large, constant P_b , $2P_v P_b \gg P_v^2$. Even though P_b^2 is larger than the homodyne term, it is constant with applied voltage. Furthermore, the low-frequency noise from P_v^2 is rejected in an ac measurement. In addition to being more sensitive, homodyne detection has the advantage of producing an output that is linear in bias voltage and a direct representation of the waveform. The EFISH and background SH signals may have different absolute phases, and the observed total SH signal (background plus EFISH) can be out of phase with the applied waveform, as shown in Fig. 4. One can also apply homodyne detection of EFISH signals to materials that do not generate SH signals at zero applied electric field, such as silicon-based devices, by combining the EFISH signal with a reference SH beam generated in a nonlinear crystal such as quartz.^{4,10}

To determine whether two-photon absorption of the laser perturbs the measurements by producing carriers, we measured the current in the devices with a picoammeter while irradiating them with the laser beam. No currents were measurable from the

UV LED (emission peak, ~ 370 nm) with 200-mW average power focused onto the UV LED. Because the ammeter current noise was approximately 100 pA, the average current in the devices was less than 100 pA. Assuming a square pulse 100 fs in duration and a repetition rate of 80 MHz, the peak currents were less than 12 μ A. For comparison, an average current of 330 nA was measured for a GaN diode with an emission peak at 400 nm. The key to low induced current is using fundamental and SH frequencies below the bandgap.

EFISH is capable of tracking voltage waveforms. Figure 4 shows EFISH detection of a square wave and a saw-toothed wave applied as a reverse bias across the UV LED. In these traces, the signal at zero bias is not removed by dual modulation. The EFISH signal is 90° out of phase with the ~ 70 -mV background SH signal. We digitized and averaged roughly 100 raw signal traces from the phototube, terminated into 100 k Ω , using a 12-bit analog-to-digital converter. With no other signal averaging or processing, the noise level is ~ 8 mV_{rms}/ $\sqrt{\text{Hz}}$. Although the waveform frequency is low in this demonstration, the EFISH technique will permit tracking of high-speed, gigahertz waveforms. Assuming appropriate detection electronics, the ultimate temporal resolution of this technique is determined by the pulse width of the laser. Applying this method noninvasively to silicon-based devices will require using a fundamental wavelength of ~ 2 μ m so the SH at ~ 1 μ m will also be below the bandgap. We are pursuing high-speed applications of EFISH to both GaN- and Si-based devices.

The research was supported by the National Science Foundation Small Business Innovation Research program under grant DMI-9960557. D. J. Kane's e-mail address is djokane@swsciences.com.

References

1. G. Lüpke, C. Meyer, C. Ohlhoff, H. Kurz, S. Lehmann, and G. Marowsky, *Opt. Lett.* **20**, 1997 (1995).
2. P. Godefroy, W. de Jong, C. W. van Hasselt, M. A. C. Devillers, and Th. Rasing, *Appl. Phys. Lett.* **68**, 1981 (1996).
3. W. Wang, G. Lüpke, M. Di Ventra, S. T. Pantelides, J. M. Gilligan, N. H. Tolk, I. C. Kizilyalli, P. K. Roy, G. Margaritondo, and G. Lucovsky, *Phys. Rev. Lett.* **81**, 4224 (1998).
4. P. T. Wilson, Y. Jiang, O. A. Aktsipetrov, E. D. Mishina, and M. C. Downer, *Opt. Lett.* **24**, 496 (1999).
5. C. Meyer, G. Lüpke, U. Emmerichs, F. Wolter, H. Kurz, C. H. Bjorkman, and G. Lucovsky, *Phys. Rev. Lett.* **74**, 3001 (1995).
6. A. Fiore, E. Rosencher, V. Berger, and J. Nagle, *Appl. Phys. Lett.* **67**, 3765 (1995).
7. A. Nahata, T. F. Heinz, and J. A. Misewich, *Appl. Phys. Lett.* **69**, 746 (1996).
8. S. Nakamura and G. Fasol, *The Blue Laser Diode* (Springer-Verlag, Berlin, 1997).
9. S. Nakamura and S. F. Chichibu, eds., *Introduction to Nitride Semiconductor Blue Lasers and Light Emitting Diodes* (Taylor & Francis, London, 2000).
10. J. I. Dadap, J. Shan, A. S. Weling, J. A. Misewich, and T. F. Heinz, *Appl. Phys. B* **68**, 333 (1999).